Multiphase stochastic model for fluidized beds

Timo Gottschalk and Herold G. Dehling
Department of Mathematics, University of Bochum, 44780 Bochum, Germany

Alex C. Hoffmann
Department of Physics and Technology, University of Bergen, Allegt. 55, 5007 Bergen, Norway

(Received 15 October 2007; published 18 March 2008)

This article introduces a type of stochastic model, which we call a multiphase stochastic model, for the particle transport in bubbling fluidized beds, making it possible to take into account the finite velocity of fluidization bubbles and also extra particle transport due to "gulf streaming." An extended analysis of experimental results for particle transport in fluidized beds with gulf streaming is given, and results from the model are compared with the experimental results, showing that the model accounts for the effects seen.

DOI: 10.1103/PhysRevE.77.031306 PACS number(s): 83.80.Fg, 02.50.Ey, 02.50.Ga, 47.61.Jd

I. INTRODUCTION

Fluidized beds are very widely used in the processing industry, and a voluminous scientific and technical literature spanning journals with the scopes of process technology, applied physics and applied mathematics is dedicated to the study and design of fluidized beds and fluidized bed processing. The issue of the flow of particles in fluidized beds is interesting to a wider audience of applied physicists interested in the dynamics of granular matter.

In this article we are interested in the vertical particle transport in bubbling gas fluidized beds. This transport is related to the movement of fluidization bubbles through the bed.

Rowe, Partridge, and Gibilaro [1,2] were the first to propose that the vertical particle motion in batch fluidized beds is governed by the following phenomena (please see the left-hand sketch in Fig. 1). (1) Transport upward in the wakes of fluidization bubbles (flow in the "wake phase") and deposition on the bed surface. (2) Transport down in the bulk (flow in the "bulk phase") to compensate for this (1 and 2 together are termed "circulation"). (3) Dispersion due to disturbance of the bed material by fluidization bubbles.

The fluidization bubbles grow as they rise due to coalescence, as indicated in the figure. Even though the total flow of empty bubble volume remains approximately constant with height in the bed, the wake fraction grows with bubble volume, so that there is a nonzero probability of a particle being caught in a wake everywhere in the bed. We note that if there is a significant pressure drop over the bed, the bubbles will also grow due to the gas expansion; this is not taken into account here, but it would not be difficult to do.

However, if the flow of fluidization bubbles is nonuniform over the bed cross section, another, and potentially more powerful, mechanism may cause vertical particle transport in the bed, namely, that of "gulf streaming." By gulf streaming bulk material (interstitial between the bubbles) is also dragged up with the bubble stream in addition to the material in the actual wakes. This flow of bulk material can be considerably larger than the wake flow, also causing a considerably faster downward bulk flow in the rest of the bed. Merry and Davidson [3] and Werther [4] were among the first to discuss this phenomenon, and it has subsequently been discussed by a number of other workers. Matsen [5] states that gulf streaming of solids is unavoidable in industrial-scale fluidized beds and that this constitutes a powerful axial mixing mechanism that is often absent in small, laboratory-scale fluidized beds with good gas distribution. Werther states that even if the gas distribution is perfect at the distributor plate, regions of high and low bubble activity will still develop higher in the bed, since the bubbles will have concentrated in the middle because of coalescence, and this will give rise to gulf-streaming effects.

Figure 1 illustrates the particle transport processes active in a bubbling fluidized bed, to the left in one with a uniform bubble distribution, and to the right in one with localized high bubble intensity, leading to gulf streaming of particles. Dehling *et al.* [6] introduced Markov chain models for the particle transport in bubbling fluidized beds based on the above-mentioned transport mechanisms of Rowe, Partridge, and Gibilaro. These models consisted of a Markov birth-death chain with an additional jump probability to the top of

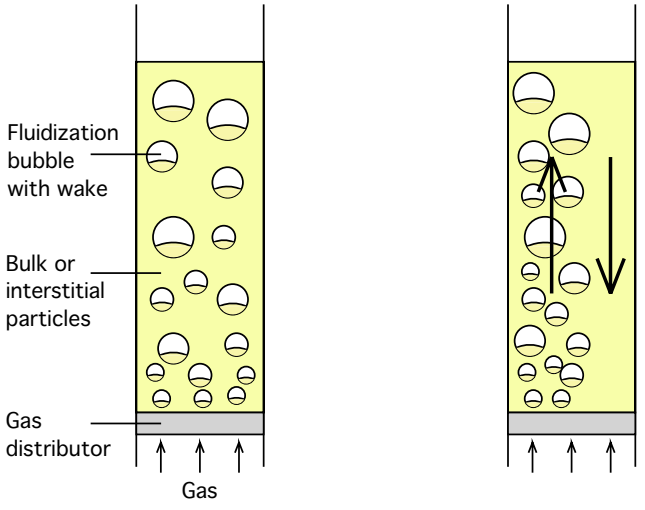

FIG. 1. (Color online) Sketches showing left: a bubbling fluidized bed with upward particle flow in bubble wakes and a compensating down-flow in the bulk and right: a bubbling fluidized bed with a region of high bubble activity leading to extra flow of particles due to gulf streaming.

the bed λ_i, describing the extra transport upward of particles caught in the wake of a rising gas bubble. Introducing such a jump to the top which amounts to admitting infinite velocity for those rising particles was certainly a model assumption of which feasibility and impact still had to be examined, although very good results had already been achieved with this approach.

Recent experiments by Dechsiri *et al.* [7–9] using a positron emission tomography camera show a quite fast rise of particles to the top but nonetheless one with finite velocity (see Fig. 5 later in this paper). A fast rise explains the quality of results of the model with jumps. However, a finite rise velocity should be included in models dealing with these kind of processes. Unfortunately a simple extension of the existing model is not possible since the information whether a particle is drifting and diffusing downward with some velocity, or moving upward with some other velocity—either in the wake of a rising gas bubble or in the upward stream caused by any "gulf streaming" taking place—is not described by the particle's position in the state space of Dehling *et al.*, which was simply the particle's location in the reactor. Thus the process loses its Markovian character.

In this paper we show how to construct a so-called multiphase Markov process capturing this additional feature while still giving easy access to the parameter of interest, namely, the spatial position of the particle. In this process a particle may, in addition to occupying any of the spatial cells into which the reactor is partitioned, be in one of two or more "phases." This is a general concept that can be used for a wide variety of applications, e.g., to model different chemical phases or different sizes in population balance modeling (PBM). The model will be developed so that it can account for the transport of material in the wakes of fluidization bubbles, gulf streaming, and exchange of material between the wake, gulf streaming, and bulk phases. The model is validated by comparing its predictions with empirical data.

Finally we will summarize a more general approach to the modeling of multiphase systems. The formulation of a stochastic model for multiphase systems presented here significantly increases the range of systems and processes that can be modeled with a Markovian model.

We note at this point that Too *et al.* [10] have published a stochastic model for the gaseous components in a fluidized chemical reactor, wherein a multiphase approach was used to describe the constituent molecules' presence in either the bubble or the dense phase of the fluidized bed, and its chemical state (reactant or product form). We will return to this when having introduced our own model to highlight similarities and differences with our approach. Kamrin and Bezant [11] recently introduced a "stochastic flow rule" for granular flows via diffusing "spots" of fluidization acting as carriers of plasticity.

Please note that in the fluidization literature, the word "phase" is normally used to refer to the bulk (or interstitial), the bubble and the wake "phases," as indicated in Fig. 1. In the context of multiphase stochastic models the word is used in a wider sense, for example, each chemical state of a particle or molecule may constitute a separate "phase."

The organization of this paper is as follows. First we introduce the multiphase stochastic model for particle transport in fluidized beds. We then show, referring also to an analysis in Chapter 8 of the monograph of Dehling, Gottschalk, and Hoffmann [12], that the results given in Ref. [9] are both qualitatively and quantitatively consistent with the existence of gulf streaming, and finally we compare the predictions of our model with the experimental results given in Refs. [9,8].

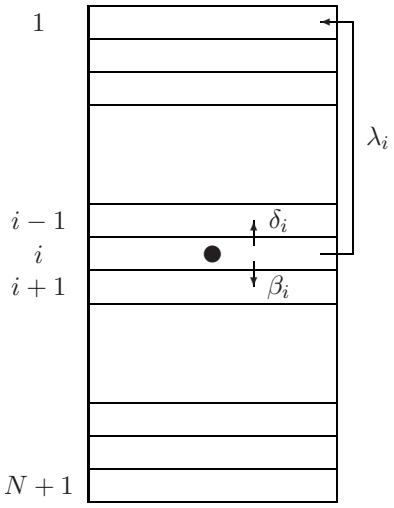

FIG. 2. Discretized fluidized bed with arrows indicating all possible transition paths for the particle located in cell i.

The discussion in this paper is given in a more complete form in Chapter 8 of Ref. [12]. The monograph of Dehling, Gottschalk, and Hoffmann [12] discusses stochastic modeling in process technology in general, including a variety of stochastic modeling techniques applied to a range of processes.

II. MULTIPHASE MODEL FOR A BUBBLING FLUIDIZED BED

We begin with the theory, harking back to the single-phase model of Dehling *et al.* [6], and then consider the model parameters in light of the physical phenomena and quantification of the parameters by comparison with experimental results.

A. Theory

We consider a bubbling fluidized bed and its stochastic model using a Markov chain as introduced by Dehling *et al.* [6] and shown in Fig. 2. We give a short recap of the Markov model of Dehling *et al.*

The bed is discretized in layers numbered from 1 to N and an absorbing state $N+1$ representing the exterior. The transition matrix $\mathbf{P}$ consists of probabilities for $2 \le i \le N$:

$$p_{i,i} = \alpha_i(1-\lambda_i) = (1-\beta_i-\delta_i)(1-\lambda_i), \quad p_{i,i+1} = \beta_i(1-\lambda_i), \quad p_{i,i-1} = \delta_i(1-\lambda_i), \quad p_{i,1} = \lambda_i$$

and

$$p_{1,1} = (1-\beta_1), \quad p_{1,2} = \beta_1, \quad p_{N+1,N+1} = 1,$$

at the boundaries. All other elements of the matrix are zero. The $p_{i,j}$ are the transfer probabilities from cell i to cell j

conditional on the particle being in cell i. The object under examination is the particle's location at each time step $n \geq 0$ denoted by the random variable X_n, which thus can take on values in $\{1,2,\ldots,N+1\}$ (its state space). λ_i denotes the probability that a particle in cell i is caught in the wake of a fluidization bubble and deposited on top of the bed, in cell 1; this constitutes a jump to the top of the bed. The position of the particle at the nth time step is governed by the probability vector $\mathbf{p}(n)$ with elements $p(n,i)$.

It is true for all time-homogeneous discrete Markov chain processes that knowing $\mathbf{p}(n-1)$, one can find $\mathbf{p}(n)$ from the recursion formula

$$p(n,j) = \sum_{i=1}^{N+1} p(n-1,i)p_{ij}$$

or in matrix notation

$$\mathbf{p}(n) = \mathbf{p}(n-1)\mathbf{P}.$$

After n time steps, we obtain the formula for the probability distribution of position of the particle at time n in terms of its initial probability distribution

$$\mathbf{p}(n) = \mathbf{p}(0)\mathbf{P}^n, \tag{1}$$

where $\mathbf{p}(0)$ is the initial condition of particle distribution at time $t=0$.

1. Beds without gulf streaming

We wish to introduce a second phase with upward movement to replace the jumps, while retaining the Markovian character of the model. To do this we have to enlarge the state space to keep track of all the necessary information to formulate a Markov chain. Thus the transition probabilities depend on the location of the particle and its present phase. As phases we distinguish in this example of a bubbling fluidized bed the "bulk phase" with ordinary downward drift with diffusion, as in the model of Dehling *et al.* [6], and a "wake phase" with the fast rise upward in the wake of a gas bubble. This gives the following state space:

$$S = \{1,2,\ldots,N\} \times \{0,1\} \cup \{(N+1,0)\}.$$

We denote the multiphase system by $(X_n)_{n\geq 0}$ now acting on S instead of $\{1,2,\ldots,N+1\}$, i.e., X_n has the form $(i,k) \in S$ for all $n \geq 0$.

We denote the particle's spatial location by the first, and its phase by the second entry of the state space variable. The entrance is thus in cell (1,0) and the absorbing cell representing the exit has the label $(N+1,0)$. The transition probabilities are

$$p_{(i,k)(i-1,k)} = \delta_i^{(k)}, \quad p_{(i,k)(i+1,k)} = \beta_i^{(k)}, \quad p_{(i,k)(i,k)} = \alpha_i^{(k)}, \quad p_{(i,k)(i,|k-1|)} = \lambda_i^{(k)}$$

and we require that

$$\alpha_{N+1}^{(0)} = 1, \quad \delta_i^{(k)} + \beta_i^{(k)} + \alpha_i^{(k)} + \lambda_i^{(k)} = 1$$

for $k \in \{0,1\}$, $1 \leq i \leq N$.

Summing up, the possible transitions are (1) Staying in the same cell, i.e., maintaining location and phase, (2) moving one cell upward, i.e., changing the location but not the phase, (3) moving one cell downward, i.e., changing the location but not the phase, and (4) Changing the phase, i.e., maintaining the location but switching the phase.

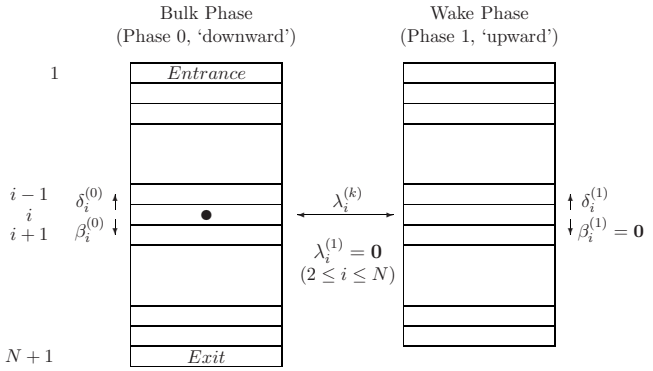

FIG. 3. Multiphase model for a fluidized bed with arrows indicating all possible transition paths for the particle located in cell $(i,0)$.

Phase 0 models the downward flow in the bulk as a drift with dispersion, and phase 1 the upward drift in the wake of rising gas bubbles. By setting

$$\beta_i^{(1)} = 0$$

for $1 \leq i \leq N$, the diffusion in this latter phase is minimized. Dispersion in an upward-flowing phase can be introduced by giving $\beta_i^{(1)}$ a value greater than zero. We shall return to this topic in the following subsection.

The transition between the two phases, representing the particle entering or leaving the wake of a gas bubble, is governed by $\lambda_i^{(k)}$. Setting

$$\lambda_i^{(1)} = 0$$

for $2 \leq i \leq N$ models that a particle will only leave the upward-moving (wake) phase at the top of the reactor. Allowing $\lambda_i^{(1)}$ to differ from zero at other axial stations in the bed, or in all cells, would model loss of particles from the wake of the rising bubbles. This would be relevant, for instance, in fluidized beds containing mixtures of particles with different densities or in baffled fluidized bed, where the baffles retain some of the wake of a rising fluidization bubble [13,14]. $\lambda_i^{(0)}$ would then similarly have to be nonzero to allow for replenishing of the wake material.

This model is shown schematically in Fig. 3. Please note that in this and the following picture, the volumes of the cells cannot be taken as representative of physical volumes.

We emphasize that this multiphase model is a Markov chain with all its advantages, in contrast to a model accounting for a finite particle rise, but involving the particle's spatial location only, which would not be Markovian. Such a one-phase model can be seen as the projection of the multiphase model on its first coordinate entry. The only way to formulate a Markovian model for the particle transport in fluidized beds involving only the particle's spatial position as state space is to allow instantaneous jumps to the surface, such as was done by Dehling, Hoffmann, and Stuut [6].

The present model with two phases is Markovian, while still allowing a finite particle velocity to the surface. By enlarging the state space such that it encodes all necessary information to completely determine the transition probabilities the process becomes a Markov process and is thus subject to the powerful theory of Markov processes.

Enlarging the state space is thus a fruitful detour to gain the desired information about the behavior of the examined system. An additional advantage is that extra information is obtained, for instance, the process keeps track of when the particle occupies each phase, i.e., the expected residence time of the particle in each phase can also be computed.

Only little literature on the subject of multiphase systems, as understood here, is available. A general and conceptual approach to modeling complex processes with multiphase Markov processes has not been presented in the literature. Such a general approach is introduced at the end of this paper. Nevertheless, some work has been done before in specific contexts. The article of Too *et al.* [10], in which the transport and chemical reaction of the gas-phase constituents in a fluidized bed reactor is modeled, stands out.

Too *et al.* divided the fluidized bed in a number of well-mixed compartments according to a fluidized bed reactor model of Mori and Wen [15] and derived a multiphase stochastic model for the constituent molecules' spatial distribution over the compartments, their chemical form and their presence in either the bubble or the interstitial phases. Our model for particle flow in the reactor differs from theirs: although space is discretized also in our model, the reactor is not divided into compartments according to a model, but the spatial particle distribution is modeled directly based on the physical particle transport mechanisms; this is a fundamental difference. Another difference is that we derive a discrete stochastic model directly rather than going over a time-continuous one, as Too *et al.* did. The multiphase Markov chain model of Too *et al.* for the gas-solids fluidized bed reactor with mixing and a chemical reactions constitutes a successful use of stochastic modeling particularly with a multiphase model.

2. Including gulf streaming

The aim of this section is to extend the above model such that the phenomenon of gulf streaming is captured. Gulf streaming is, as mentioned, caused by a cross-sectionally nonuniform bubble flow, inducing an extra upward flow in one part of the bed and a corresponding downward flow somewhere else in the bed (see Fig. 1). A consequence of gulf streaming is thus that much more material is transported from the bottom to the top than that transported in bubble wakes alone, and this gives rise to a correspondingly enhanced downward bulk flow.

Gulf streaming is a common effect, especially in large industrial beds and will often be the dominating axial mixing mechanism compared to mixing by the flow of wake material [3–5]. In the section below, when analyzing experimental results for particle transport in a bed with gulf streaming, we will find that only about 0.0224 m/s of the total solids upflow per unit area of about 0.263 m/s is due to flow in the actual bubble wakes.

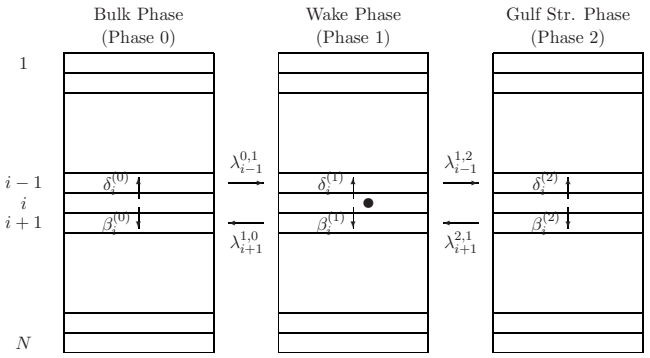

FIG. 4. Extended multiphase model for a fluidized bed with the particle located in cell $(i,1)$ and arrows indicating some possible transition paths.

From this point on we consider a closed reactor without an exit and delete the state $(N+1,0)$ from the state space of the multiphase model. To incorporate the possible exchange of wake material and bulk flow we set the parameter that governs this exchange $\lambda_i^{(k)}>0$. In other words the fraction of wake material in a rising gas bubble that leaves the gas bubble and joins the bulk flow at location i is greater than zero, and, conversely, the wake is replenished from the surrounding bulk.

Including gulf streaming in the model requires that we enlarge the state space again. We enlarge the state space to

$$S=\{1,2,\ldots,N\}\times\{0,1,2\}.$$

In this, the first entry between 1 and N still encodes the particle's location and the second entry encodes its phase, which may now be either phase 0 with downward bulk flow with minimal dispersion or phase 1 with upward flow in the wake of a rising gas bubble with minimal dispersion or phase 2 with upward flow between the bubbles via gulf streaming with dispersion.

Phase 0 models movement in the part of the reactor without (or with very little) bubble activity, and therefore the flow there exhibits only minimal dispersion. More dispersion takes place in phase 2 due to disturbance of the up-going stream by the fluidization bubbles "carrying" it. The corresponding transition probabilities are now given as

$$p_{(i,k)(i-1,k)}=\delta_i^{(k)},\quad p_{(i,k)(i+1,k)}=\beta_i^{(k)},\quad p_{(i,k)(i,l)}=\lambda_i^{k,l}$$

and we require

$$\delta_i^{(k)}+\beta_i^{(k)}+\sum_{l=0}^{2}\lambda_i^{k,l}=1 \tag{2}$$

for $k,l\in\{0,1,2\}$, $1\le i\le N$. The probability to stay in a given cell $p_{(i,k)(i,k)}$ is thus denoted by $\lambda_i^{k,k}$.

The possible transitions are the same as in the model in Sec. II. We picture the situation in Fig. 4.

This completes the formulation of the model for a bubbling fluidized bed with gulf streaming. The transition probabilities now have to be assigned to be consistent with the

TABLE I. Overview of constraints on transition probabilities

	up/down	Transition to wake/bulk ($l\in\{0,1\}$)	Transition to gulf streaming
Bulk flow	$\delta_i^{(0)}=0$		$\lambda_i^{0,2}\sim 0$ for $i_0<i<i_1$
Wake flow	$\beta_i^{(1)}=0$		$\lambda_i^{1,2}\sim 0$ for $i_0<i<i_1$
Gulf streaming up	$\beta_i^{(2)}=D_i+\frac{1}{2}v_i$, $\delta_i^{(2)}=D_i-\frac{1}{2}v_i$	$\lambda_i^{2,l}\sim 0$ for $i_0<i<i_1$	

physical processes. The parameters $\lambda_i^{k,l}$ governing the interchange between the phases are rather difficult to quantify from experimental evidence.

B. Relating the model parameters to the physical phenomena

Following Dehling *et al.* [6], we describe the particle transport in each of the phases by a velocity $\tilde{v}$ in m/s describing the flow of the particles in the phase and a (Fickian) dispersion coefficient $\tilde{D}$ describing the dispersion of the particles due to the disturbance created by fluidization bubbles. This equals half of the mean squared particle displacement per second.

The physical velocities and dispersions have to be converted to dimensionless ones. For given spatial and temporal discretizations Δ (the height of a spatial cell in m) and ϵ (the length of a time step in s) the conversion formulas are

$$v\frac{\Delta}{\epsilon}=\tilde{v}(\text{in m/s}),\quad D\frac{\Delta^2}{\epsilon}=\tilde{D}(\text{in m}^2/\text{s}), \tag{3}$$

where v and D are the dimensionless velocity and dispersion coefficients and $\tilde{v}$ and $\tilde{D}$ their physical equivalents. This yields a mean displacement of

$$(\Delta\times\beta_i^{(k)}-\Delta\times\delta_i^{(k)})\frac{1}{\epsilon}=(\beta_i^{(k)}-\delta_i^{(k)})\frac{\Delta}{\epsilon}$$

and a mean squared displacement of

$$(\Delta^2\times\beta_i^{(k)}+\Delta^2\times\delta_i^{(k)})\frac{1}{\epsilon}=(\beta_i^{(k)}+\delta_i^{(k)})\frac{\Delta^2}{\epsilon}$$

for a given cell (i,k).

Dispersion enters into the model by setting the mean squared displacement equal to two times the dispersion coefficient. This is a reasonable simplification since the physical dispersion, usually seen as the variance, which is given by mean displacement squared subtracted from mean squared displacement, is approximated by its dominating term: the mean squared displacement. A corollary is that true plug flow can only be modeled in one way, namely, by setting the corresponding transition probability δ or β equal to 1 and choosing the time and space discretization such that $\Delta/\epsilon=\tilde{v}$ s/m. We are not free to choose our time and space discretization in this way here, but can only minimize dispersion in the phases where we consider that negligible dispersion takes place.

Thus the dimensionless velocity (or mean displacement per time step) and quadratic displacement at location i in the kth phase become

$$v_i=\beta_i^{(k)}-\delta_i^{(k)},\quad 2D_i=\beta_i^{(k)}+\delta_i^{(k)}. \tag{4}$$

We consider the transition probabilities within each phase first and those between the phases thereafter.

Bulk flow. In the bulk flow we need to minimize dispersion and ensure a downward flow. Setting the flow parameter $\delta_i^{(0)}$ to be zero allows no upward flow in the bulk and minimizes dispersion.

Wake flow. Analogous to the bulk flow, the wake flow has minimal dispersion and there is no downward movement. Thus the wake flow parameter $\beta_i^{(1)}$ is set to zero.

Gulf streaming upward. Upward gulf streaming exhibits dispersion, since this is the region through which most of the bubbles flow. Thus we impose that $\beta_i^{(2)}=D_i+\frac{1}{2}v_i$ and $\delta_i^{(2)}=D_i-\frac{1}{2}v_i$ to generate a dispersion with dimensionless mean squared displacement of $2D_i$ and a dimensionless velocity of v_i, conditioned on the particle remaining in the phase, at location i.

Between the phases the following constraint is made. Flow between the gulf streaming phase and all other phases almost only takes place in the upper and lower regions of the reactor. Thus the parameters $\lambda_i^{k,l}$ have to be very small if $k=2$ or $l=2$ and $i\in\{i_0+1,\ldots,i_1-1\}$ for some $1\le i_0\le i_1\le N$. Then $\{1,2,\ldots,i_0\}$ constitutes the upper and $\{i_1,\ldots,N\}$ the lower part of the reactor where most transitions involving the gulf streaming phase take place. No other restrictions on the transition probabilities $\lambda_i^{k,l}$ are made. Table I gives an overview of the constraints above.

If the particles in the reactor are incompressible, which is the same as saying that, on average, the void fraction in all of the spatial cells remains constant in time, no mass can accumulate in any given cell. Then the mass balance equation

$$\sum_{i=1;k\in\{0,1,2\}}^{N}p_{(i,k),(j,l)}=\delta_{j+1}^{(l)}+\beta_{j-1}^{(l)}+\sum_{k=0}^{2}\lambda_j^{k,l}=1 \tag{5}$$

must be satisfied for all $(j,l)\in\{1,\ldots,N\}\times\{0,1,2\}$. This completes our adaptation of the multiphase model to a fluidized bed with gulf streaming. In order to quantify the model parameters, specifically v and D, we will now further analyze the experimental results for particle motion in a bubbling fluidized bed that exhibited gulf streaming, given by Dechsiri *et al.* [9].

C. Experimental results for fluidized beds with gulf streaming

In this section we give a further analysis of results emanating from a positron emission tomography (PET) study of the motion of a particle in a bubbling fluidized bed that exhibited gulf streaming. The entire PET study is reported in

TABLE II. Physical properties of the particles used

	Lewatit MP500	FCC catalyst
Average particle size [μm]	470	79.5
Envelope density [kg/m^3]	1060	1464
Sphericity [−]	1	0.9
ϵ_{mf}	0.42	0.45
U	0.130	0.01
U_{mf} measure [m/s]	0.116	0.004

three articles [7–9], where all the details of the experimental and analysis techniques are given. A more detailed discussion of the analysis is given in Chapter 8 of Ref. [12].

In Ref. [9] the motion of a single, radioactive particle was followed in 3D. A macroporous anion exchange resin, Lewatit MP500 was used, the physical properties of which are given in Table II. In the table U is the superficial gas velocity with which the powder was fluidized, and U_{mf} that required just to fluidize the powder; we use the word "superficial" to mean the actual velocity of the interstitial gas multiplied by the void fraction ϵ, of the bed. In another paper [8] pulses of radioactive particles in a bed of fluidized catalytic cracking (FCC) catalyst were followed. The properties of these particles are also given in Table II.

In both sets of experiments a bed vessel with an inner diameter of 15 cm and a height of 35 cm was used. Analyses showed [7,12] that the position of the particle could be determined to within one cubic mm once per ms and the scatter could be further reduced without loosing information about the real movement of the particle by averaging the positional data over about 20 ms. The paths of the particle are therefore very accurately determined.

The motion of a tracer particle in a Cartesian coordinate system with the origin in the center of the camera's cylindrical sensing zone and the y axis vertically upward is shown in Fig. 5. The particle can be seen generally to rise faster than it descends, consistent with quick rise associated with the bubble phase and slower descent in the bulk. However, when computing the expected bulk descent velocity under the given operating conditions using relations for (a) the total bubble flow, (b) the bubble size, and (c) the bubble velocity, this expected descent velocity turns out to be much smaller than the descent velocity seen in the figure. This indicates that there is far more vertical transport than can be accounted for by transport in bubble wakes alone. Figure 6 shows a plot of the particle velocities measured over a cross section in the middle of the bed.

This figure clearly shows that the particle circulates in the bed, rising rapidly—but with a large spread in the

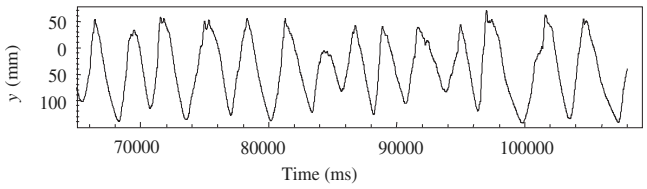

FIG. 5. Time series of the tracer particle's y position (height in bed).

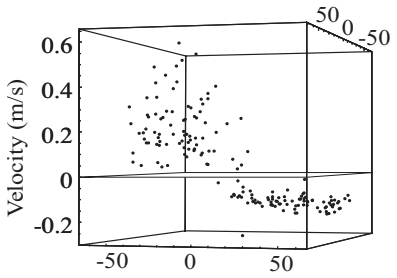

FIG. 6. 3D plot of the particle velocities over a cross section in the middle of the bed.

velocities—in one part of the bed and descending more slowly in another part. This indicates "gulf streaming" (see Fig. 1). This effect is probably due to less-than-optimal gas distribution in this laboratory bed. However, gulf streaming is present in almost all large industrial beds, if not due to inferior gas distribution over the cross section of the distributor, then due to the fluidization bubbles concentrating near the axis as a consequence of coalescence.

Consistent with this we assume that the bed cross section can be split in two regions: one with a strong bubble activity and a generally upwardly directed particle flow, either in the wakes of fluidization bubbles, or in the material between the bubbles, and another with downward particle flow in which the bubble activity is low or absent. Figure 7, wherein the starting points of upward particle paths are shown, support this view, and seems to indicate that the upward flow takes up about 1/3 of the bed cross section.

Figure 8 shows a frequency plot for the particle velocities shown in Fig. 6. Two local maxima at about −0.125 m/s and +0.2 m/s are clear, and a few times the tracer particle can be seen to have passed the middle with a velocity of +0.5–+0.6 m/s. This leads us to assume the velocity of descent, which we can already identify with $v^{(0)}$ from the previous section, is about 0.125 m/s, and the velocity of ascent in the bulk phase between the fluidization bubbles $v^{(2)}$ is 0.2 m/s while the velocity of the bubble wakes, which follow the fluidization bubbles $v^{(1)}$ may be 0.5−0.6 m/s. In chapter 8 of

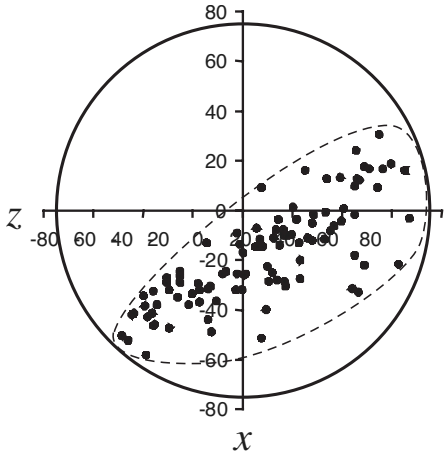

FIG. 7. Starting points for upward particle paths in the bed. The figure is redrawn from Ref. [9]. The cross-sectional region containing all the starting points is indicated by a broken line.

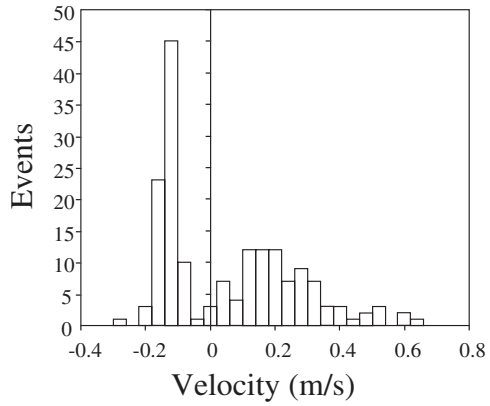

FIG. 8. Frequency plot for the velocities shown in Fig. 6.

Ref. [12] the data given in Ref. [9] are analyzed further to show that these values are reasonable in light of what is known about particle transport velocities in bubbling fluidized beds.

D. Quantification of the model parameters

We now need to find the dimensionless velocity v_i, dispersion coefficient D_i, and phase transition rates $\lambda_i^{k,l}$ to calculate the transition probabilities according to the following scheme:

$$\beta_i^{(k)} = D_i + \tfrac{1}{2}v_i, \quad \delta_i^{(k)} = D_i - \tfrac{1}{2}v_i, \quad \lambda_i^{k,l} = \bar{\lambda}_i^{k,l} \quad (1 \le i \le N; k,l \in \{0,1,2\}; k \ne l).$$

The dimensionless phase transition rates $\bar{\lambda}_i^{k,l}$ are given as

$$\bar{\lambda}_i^{k,l} = \epsilon \tilde{\lambda}_i^{k,l},$$

the physical transition rates $\tilde{\lambda}_i^{k,l}$ having SI units of $1/\mathrm{s}$. Thus a particle in cell (i,k) has a probability of $\epsilon\tilde{\lambda}_i^{k,l}$ to change from its current phase k to phase l during a time period of length ϵ.

To calculate the dimensionless velocities and dispersion coefficients v_i and D_i from Eq. (3) we need to quantify the spatial and the temporal discretization steps Δ and ϵ. We obtain Δ as the quotient of height of the bed h and number of cells N

$$\Delta = \frac{h}{N}.$$

Choosing $\epsilon = \Delta$ ensures a fine discretization and has the advantage that $\mathrm{m/s}$ converts to Δ/ϵ one to one. This results in each time step having the length $\epsilon = \frac{h}{N}$. The conversions between physical and dimensionless parameters are then, according to Eq. (3), obtained as

$$v_i = \tilde{v}_i \frac{\epsilon}{\Delta} = \tilde{v}_i \frac{s}{m}$$

and

$$D_i = \tilde{D}_i \frac{\epsilon}{\Delta^2} = \tilde{D}_i \frac{N}{h}\frac{\epsilon}{\Delta} = \tilde{D}_i \frac{N}{h}\frac{s}{m}.$$

In these equations, and hereinafter, the factor s/m denotes a factor of unity, namely, ϵ/Δ with the SI unit $\mathrm{s/m}$.

From Sec. II C and Fig. 8 we obtain for the velocities $v^{(k)}$ corresponding to the three phases

$$v^{(0)} = 0.125 \ \mathrm{m/s}, \quad v^{(1)} = 0.577 \ \mathrm{m/s}, \quad v^{(2)} = 0.2 \ \mathrm{m/s}.$$

The dispersion is minimal in phases 1 and 2 and for phase 3 the following relation, developed in Dehling *et al.* [6] on basis of the particle drift profiles measured by Tanimoto *et al.* [16]:

$$\text{Mean squared displacement} = 2\tilde{D} = 0.2089 D_b (1 - f_w)^{1/3} (U - U_{mf})$$

with D_b the bubble diameter and f_w the wake fraction (see Ref. [12]), gives

$$\tilde{D}^{(2)} = 1.7 \times 10^{-4} \ \mathrm{m^2/s}.$$

Based on the interpretation of Fig. 8 given above and in Ref. [12] the transition rates from the downward bulk flow to the upward gulf streaming flow and the upward flow in the bubble wakes have a ratio of 0.2 to 0.0343. This gives

$$\frac{\sum_{i=i_1}^{N} \lambda_i^{0,1} \pi(i,0)}{\sum_{i=i_1}^{N} \lambda_i^{0,2} \pi(i,0)} = \frac{0.2}{0.0343}, \tag{6}$$

where $\pi(i,k)$ denotes the invariant distribution of $(X_n)_{n\ge 0}$ evaluated for cell (i,k). Assuming the parameters $\lambda_i^{0,1}$ and $\lambda_i^{0,2}$ to be constant for $i \in \{i_1, \ldots, N\}$ and using the fact that the two transfer probabilities must sum to 1 simplifies Eq. (6) to

$$\lambda_N^{0,1} = 0.854, \quad \lambda_N^{0,2} = 0.146$$

for the bottom of the reactor, while

$$\frac{\lambda_i^{0,1}}{\lambda_i^{0,2}} = 5.83$$

still has to hold for $i_1 \le i \le N-1$. It is worthwhile to note that Eq. (6) becomes

$$\frac{\sum_{i=i_1}^{N} \lambda_i^{0,1}}{\sum_{i=i_1}^{N} \lambda_i^{0,2}} = \frac{0.2}{0.0343}$$

if π is the uniform distribution. Physical considerations, namely the absence of segregation in the fluidized bed, lead to the conclusion that the invariant (stationary) distribution is given by the uniform distribution. This justifies the simplification made above of Eq. (6) using the uniform distribution.

The height of the bed in fluidized state is 0.22 m. We divide the bed in $N=440$ equisized cells yielding $\Delta = 0.0005$ m and $\epsilon = 0.0005$ s. The transition parameters for exchange between the phases $\lambda_i^{k,l}$ and the regions of exchange between gulf streaming and bulk delimited by i_0 and i_1 are difficult to determine and those parameters not dis-

cussed above, such as the values of i_0 and i_1, set as reasonable fits. The resulting transition probabilities are

$$\delta_i^{(0)} = 0 \quad \text{for all } 2 \le i \le N,$$

$$\delta_i^{(1)} = \tilde{v}^{(1)} \frac{s}{m} = 0.577 \quad \text{for all } 2 \le i \le N,$$

$$\delta_i^{(2)} = \left(\frac{N}{h} \tilde{D}^{(2)} - \frac{1}{2} \tilde{v}^{(2)} \right) \frac{s}{m} = 0.44 \quad \text{for all } 2 \le i \le N,$$

$$\beta_i^{(0)} = \tilde{v}^{(0)} \frac{s}{m} = 0.125 \quad \text{for all } 1 \le i \le N-1,$$

$$\beta_i^{(1)} = 0 \quad \text{for all } 1 \le i \le N-1,$$

$$\beta_i^{(2)} = \left(\frac{N}{h} \tilde{D}^{(2)} + \frac{1}{2} \tilde{v}^{(2)} \right) \frac{s}{m} = 0.24 \quad \text{for all } 1 \le i \le N-1,$$

$$\lambda_i^{0,1} = 0 \quad \text{for all } 2 \le i \le i_1 - 1,$$

$$\lambda_i^{0,1} = 0.0007 \quad \text{for all } i_1 \le i \le N-1,$$

$$\lambda_i^{0,2} = 0.00075 \quad \text{for all } 2 \le i \le i_0,$$

$$\lambda_i^{0,2} = 0.000078 \quad \text{for all } i_0 < i < i_1,$$

$$\lambda_i^{0,2} = 0.004 \quad \text{for all } i_1 \le i \le N-1,$$

$$\lambda_i^{1,0} = 0 \quad \text{for all } 2 \le i \le N-1,$$

$$\lambda_i^{1,2} = 0 \quad \text{for all } 2 \le i \le N-1,$$

$$\lambda_i^{2,0} = 0.005 \quad \text{for all } 2 \le i \le i_0,$$

$$\lambda_i^{2,0} = 0.000061 \quad \text{for all } i_0 < i < i_1,$$

$$\lambda_i^{2,0} = 0 \quad \text{for all } i_1 \le i \le N-1,$$

$$\lambda_i^{2,1} = 0 \quad \text{for all } 2 \le i \le N-1,$$

$$\lambda_1^{1,0} = 1,$$

$$\lambda_N^{0,1} = 0.854,$$

$$\lambda_N^{0,2} = 0.146,$$

$$\lambda_1^{2,0} = 0.76,$$

with $i_0=80$ and $i_1=400$. All other transitions except for $\lambda_i^{k,k}$ are set to zero. The one-step return probabilities $\lambda_i^{k,k}$ are chosen in such a way that Eq. (2) holds. The high value of N is due to the large variations in the dispersion coefficients and the velocities and the requirement that all transition probabilities must be nonnegative, i.e., here $\frac{N}{h}\tilde{D}^{(2)} - \frac{1}{2}\tilde{v}^{(2)} \ge 0$.

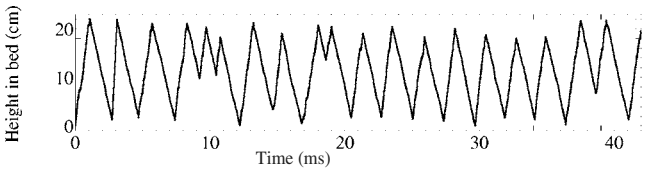

FIG. 9. Time series of the tracer particle's y position (height in bed) according to the model; please compare with the experimental results shown in Fig. 5.

III. MODEL VALIDATION WITH DATA

Using the model and data presented above, a simulation of the path of a single particle starting in cell $(N,0)$ at the bottom of the bed is computed for 42 s with MATLAB. This simulation should be compared to the experimental results shown in Fig. 5 (see Fig. 9). Comparison of simulation and experiment provides the following information.

The experimental results show 14 cycles, while the simulation shows 16. The latter is consistent with expectation, since the downward velocity used in the model is 0.125 m/s and an averaged upward velocity is $(0.146 \times 0.577 + 0.854 \times 0.2)$ m/s=0.255 m/s, yielding a mean cycle time of $(0.22/0.125 + 0.22/0.255)$ s=2.62 s and a mean number of cycles of $42/2.62 \approx 16$, disregarding any phase changes.

The maxima of 13 of the 14 passages in the experiment lie in the upper 4 cm of the bed, while 11 of 14 minima are in the lower 2 cm of the bed. For the simulations both counts were 12 of 16.

There are four phase transitions changing from a downward to an upward flow and two in the other direction in the middle section of the reactor in the experiment. The simulated path exhibits four changes from downward to upward flow and one change from up-to downward flow. All other phase changes take place in the upper 4 and lower 2 cm of the bed. Also in this respect simulations and experiment are consistent.

The simulated path is much straighter and sharper around the extrema than the experimental one. This is no surprise, since the velocities in the model are kept constant throughout the whole reactor. Obviously they should be adjusted at top and bottom regions to decrease in the neighborhoods of the extrema.

In conclusion it can be said that the experimental and simulation results agree very well. Qualitatively the simulation captures all the essential features of the observed particle movement. Quantitatively simulation and experiment agree closely although the velocities in the model are somewhat larger than those for the observed path. The simulation still lacks minor characteristics. This could be expected, and in some cases it was purposefully ignored in the effort to keep the model simple. The most pressing issue is quantification of the phase transition parameters.

A. Comparison with Pulses of Tracer Particles

In addition to the single-particle tracing pulses of radioactive particles were followed in the FCC catalyst powder. These experiments are discussed in detail by Dechsiri *et al.*

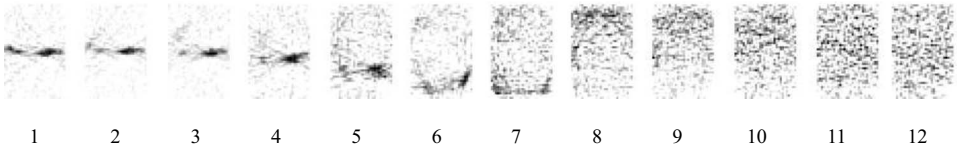

FIG. 10. PET images showing the spread of a pulse initially positioned in the middle of the fluidized bed. The time in seconds is given below the images. Details of the experimental and analysis method are given in Ref. [8].

[8], and we will compare them with predictions of the multiphase model here.

Figure 10 shows the dispersion a pulse of particles initially arranged in the middle of the bed. The time in seconds is given under the images. After an initial slight rise seen at 2 s, due to the fluidization gas being turned on, it can be seen how the main part of the layer moves down while being slightly dispersed. This descent begins at 3 or 4 s, when the fluidization bubbles "hit" the layer. Once the layer reaches the bottom of the bed it is rapidly, and under significant dispersion, brought to the top of the bed, again beginning a descent. Careful scrutiny of the images shows that a smaller part of the layer separates and initially moves up under strong dispersion.

According the law of large numbers the probability distribution for the position of one particle represents the way in which a pulse of infinitely many particles will distribute in the bed. Calculations of the vertical probability distribution of a particle starting at the top of the bed using our model, but with values for v and D fitted to these experiments, are shown in Fig. 11.

The profiles in Fig. 11 were calculated by raising the transition matrix to a power defining the output time and multiplying the starting distribution vector from the left as shown in Eq. (1). Thus no simulations are involved here, only calculation. This gives more exact results and a far lower computer-processing time than when using simulations, e.g., Monte Carlo Markov chain methods.

The start of the calculations at time 0 s, should be compared with the time at which the fluidization bubbles hit the layer in the experiments, which is sometimes between 3 and 4 s. Figure 11 shows that the particles starting in the middle of the reactor move either upward or downward in three pulses. The by far largest pulse moves downward, the two

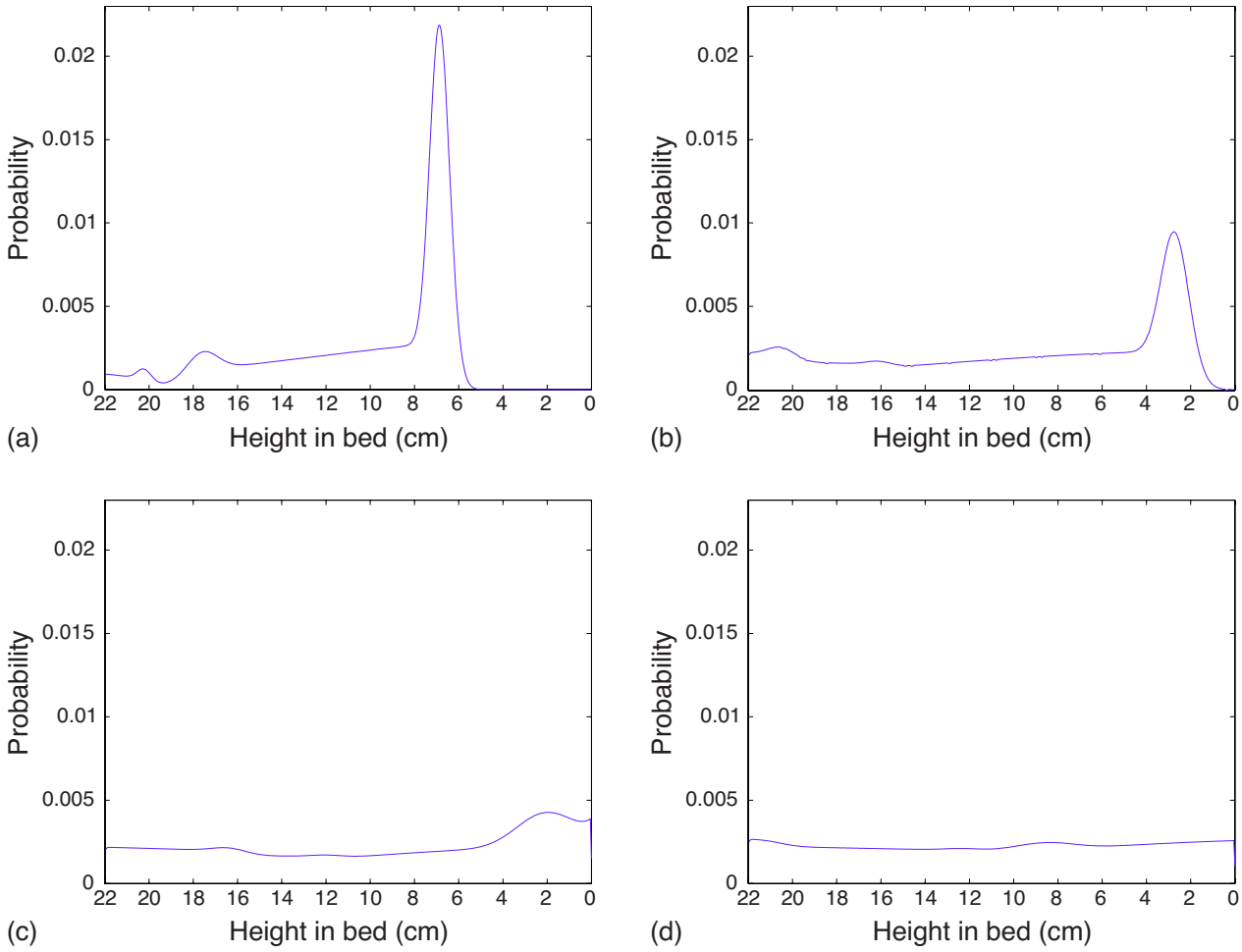

FIG. 11. (Color online) Probability distribution for the particle's vertical position at 1, 2, 3, and 4 seconds, reflecting the way a pulse of particles will distribute over the bed with time.

smaller ones upward. This is in accordance with the model setup. The two smaller pulses are the particles already in the wake phase and the upward gulf-streaming phase when the simulation is started. The latter of these two, which is the second-largest pulse moving upward less quickly, is equivalent to the small upward-moving pulse seen (mainly to the left in the bed) in the experiments.

The velocities agree with those seen in Fig. 10. The downward movement of the pulse in the bulk is constant in time and it needs about 3 s to reach the bottom, similarly to what is seen in Fig. 11. Just over one second after the fluidization gas is turned on the upward moving, second-largest pulse reaches the top of the bed, and the dispersion in this is much faster than in the down-going one. This is also seen in both the experimental and the modeling results.

In spite of all the common features in experimental and model results mentioned above they differ slightly in that the main pulse is dispersed much faster when brought to the top in the model simulations than in the experiments. A considerable amount of work remains, one important aspect is quantifying the parameters for the phase transitions. Moreover Eq. (5) has not yet been used in the setup of the model and should improve its quality when implemented.

IV. CONCLUDING REMARKS, THE ABSTRACT MULTIPHASE SYSTEM

As is usual in stochastic modeling in process technology the experimenter first has to identify the physical driving forces and mechanisms, which must be considered when formulating the model. Care has to be taken that the model remains tractable while reflecting correctly the physical mechanisms at work. The use of a multiphase system is indicated if the evolution of the system $(X_n)_{n\geq 0}$ from one time step n to the next $n+1$ $(X_n \rightarrow X_{n+1})$ cannot be derived using one parameter, i.e., state, alone but a (finite) number of these must be considered, or if the object of interest may exist in different states (chemical etc.). After this has been done, two crucial steps are the specification of the state space and the transition probabilities.

The state space includes the information of interest, e.g., the particle's spatial location or the number of particles in some class. It also has to reflect that the transition probabilities can only depend on the present state X_n and no other states in the past. In the case of a multiphase system, information about the aspect of interest does not suffice to generate a Markovian process, more information is required for formulating a matrix of transition probabilities that depend on the present state alone, i.e., one that can be computed with the information at hand. Therefore the state space has to be enlarged, beginning with the information of interest, until it contains all information necessary to formulate a Markovian process. In our case the information of interest is the particle's spatial location, which is not enough to formulate the transition probabilities, since we also need to know the phase the particle occupies. We therefore have to enlarge the state space to include information about the present phase to formulate the transition probability matrix—and thus the Markovian process—on basis of the state alone.

Subsequently the transition probabilities have to be assigned. They determine the behavior of the system and continue the implementation of physical processes in the model. The transition probabilities need to be consistent, i.e., greater than 0 and summing up to 1. Particular attention should be given to the transition probabilities between phases because these do not exist in simpler models. For practical use quantification of the model parameters, especially the transition probabilities, which can be a difficult task, is of uttermost importance. Qualitative knowledge about the system should enter the choice of the transition parameters as well. One can think of (local) mass balances or (known) long-time behavior, e.g., knowledge of the invariant distribution.

Finally the theory of Markov chains can be applied with full force using preliminary results. The transition matrix and its iterates give predictions of the system after some time steps when starting from an initial setup [Eq. (1)]. Long time behavior of the system can be deduced by considering the eigenvalues and eigenvectors of the transition matrix. Residence time distributions are available when applying techniques from Refs. [12,17]. In spite of us having shown a number of simulations in this paper, it should not be forgotten that information about Markov chain models can be exactly computed via matrix manipulations which is more elegant and usually significantly faster and more convenient than running simulations.

In spite of their potential for incorporating a huge variety of physical processes, stochastic models depend on empirical quantitative input, for instance, here about fluidization bubble properties, the fraction of cross-sectional area taken up by upward particle flow and the vertical velocities of particles. In spite of the physical processes being complex, and perhaps even nonlinear (such as likely gulf streaming, which, once initiated, is likely to be at least somewhat self-amplifying) they can still be reflected in the transfer probability matrix once such quantitative information is available.

Purely physical simulations, such as "granular dynamics" simulations, carry the promise of predicting all details of the process without such quantitative input. However, the practical realization of this promise is quite far in the future, at least for the type of process discussed here. Such simulations are at present only possible with a very limited number of particles, and the modeling of large fluidized bed is only possible with "continuum models," which also require input from either experiment or small-scale simulations [18].

Markov chain-based models are not necessarily stationary (time-homogeneous), the transition probability matrix may vary in time. Further development of more advanced models wherein the transfer probability matrix varies, possibly in response to variations in the position probability vector, may provide the means to incorporate some of the complex effects mentioned above, reducing the need for quantitative input to stochastic models.

[1] P. N. Rowe and B. A. Partridge, *Interaction Between Fluids and Particles* (Institute of Chemical Engineers, London, 1962), pp. 135–142.
[2] L. G. Gibilaro and P. N. Rowe, Chem. Eng. Sci. **29**, 1403 (1974).
[3] J. M. D. Merry and J. F. Davidson, Trans. Inst. Chem. Eng. **81**, 361 (1973).
[4] J. Werther, AIChE Symp. Ser. **141**, 53 (1973).
[5] J. M. Matsen, Powder Technol. **88**, 237 (1996).
[6] H. G. Dehling, H. W. Stuut, and A. C. Hoffmann, SIAM J. Appl. Math. **60**, 337 (1999).
[7] A. C. Hoffmann, C. Dechsiri, F. van der Wiel, and H. G. Dehling, Meas. Sci. Technol. **16**, 851 (2005).
[8] C. Dechsiri, E. A. van der Zwan, H. G. Dehling, and A. C. Hoffmann, AIChE J. **51**, 791 (2005).
[9] C. Dechsiri, A. Ghione, F. van der Wiel, H. G. Dehling, A. M. J. Paans, and A. C. Hoffmann, Can. J. Chem. Eng. **83**, 88 (2005).
[10] J. R. Too, R. O. Fox, L. T. Fan, and R. Nassar, AIChE J. **31**, 992 (1985).
[11] K. Kamrin and M. Z. Bazant, Phys. Rev. E **75**, 041301 (2007).
[12] H. G. Dehling, T. Gottschalk, and A. C. Hoffmann, *Stochastic Modeling in Process Technology*, Vol. 211 of Mathematics in Science and Engineering (Elsevier, Amsterdam, 2007).
[13] J.-J. van Dijk, A. C. Hoffmann, D. Cheesman, and J. G. Yates, Powder Technol. **98**, 273 (1998).
[14] C. Dechsiri, J. C. Bosma, A. C. Hoffmann, G. Hui, and H. G. Dehling, in *Proceedings of PARTEC 2001, International Congress for Particle Technology* (NünbergMesse GmbH, Nünberg, 2001).
[15] S. Mori and C. Y. Wen, in *Fluidization Technology*, edited by D. L. Keairns (Hemisphere, Washington, DC, 1976).
[16] H. Tanimoto, S. Chiba, T. Chiba, and H. Kobayashi, J. Chem. Eng. Jpn **14**, 273 (1981).
[17] T. Gottschalk, H. G. Dehling, and A. C. Hoffmann, Chem. Eng. Sci. **61**, 6213 (2006).
[18] N. G. Deen, M. V. Annaland, and J. A. M. Kuipers, Appl. Math. Model. **30**, 1459 (2006).